



A variational formulation for smeared fixed-crack models

Francesco Freddi, Gianni Royer-Carfagni

University of Parma, Dep. of Civil-Environmental Engineering and Architecture, Italy.

francesco.freddi@unipr.it, gianni.royer@unipr.it

ABSTRACT. The localization of large strains in very thin bands, smeared view of fractures, is associated with the minimization of a two-field functional similar to that proposed by Bourdin-Francfort-Marigo (2000). Here, we consider that fractures may be different-in-kind because of the material microstructure which, once loosened, allows to accommodate only a particular class of inelastic deformations (e.g., dilatation, slipping, cavitation). By varying the form of such class in the corresponding variational problem, various responses can be captured incorporating the idea of cleavage, deviatoric, combined cleavage-deviatoric and masonry-like fractures. The model is numerically implemented using a standard finite-element discretization, adopting an alternate minimization algorithm with an inequality constraint to impose crack irreversibility.

KEYWORDS. Fracture mechanics; Damage mechanics; Variational calculus; Fixed crack model.

INTRODUCTION

In continuum mechanics the formation of fractures is naturally associated with discontinuities in the deformation field. This gives two main difficulties: on the one hand, the continuum description becomes complicated because the deformation is not differentiable in the classical sense; on the other hand, the location of the discontinuity points is unknown *a priori*, hence the mathematical classification of *free-discontinuity* problems. In a fundamental paper [1], Francfort and Marigo first introduced a variational approach to fractures through the minimization of a strain energy functional, composed of a bulk and a surface energy term *à la* Griffith, adding proper constraints to impose that fractures are irreversible. The variational problem is set in a suitable class of functions for the deformation field which allows for discontinuity points, so that the location of the cracks is not given a priori but directly deduced from energy minimization. Later on the same authors, together with Bourdin [2], proposed a variational approximation of the free-discontinuity problem with a *regularized* two field functional, where one field is representative of the macroscopic displacement in the body, while the other one, say s , plays the role of a damage parameter varying between 0 and 1 ($s = 0$ in a fractured zone and $s = 1$ away from it), associated with the macroscopic decay of the material elastic moduli. This formulation leads to a pseudo spatial-dependent theory since it allows for spatial gradients of the damage parameter to affect the value of the stored energy functional. In the regularized approach fracture is not sharp, but represented by the occurrence of very large strains in very thin bands. The relationship with the parent free discontinuity problem is mathematically justified through a particular type of variational convergence referred to as Γ -convergence [3]: by extending a result for the Mumford-Shah functional in problems of image-segmentation [4], it was proved in [2] for the case of antiplane shear that as a characteristic parameter goes to zero, the regularized functional Γ -converges to the Griffith-like functional of [1], i.e., the strain peak converges to a sharp discontinuity. Many other contributions have been proposed since then and the reader is referred to [5] for an updated survey of the relevant Literature.

In a more technical language [6], the model of [1] is in the class of *fixed-crack* formulations, because the position and orientation of a crack cannot be modified during the loading history. In addition to this characterization, the model of [2] can be considered a *smeared* crack formulation, because the occurrence of individual cracks is represented, rather than by discontinuities of the displacement field, by the localization of very large strains in thin bands. This process is driven by a localized material weakening interpreted by the *damage* parameter s .



We take this view and consider the formulation of [2] as an autonomous *smeared fixed-crack model*, governed by a *pseudo-spatial-dependent* nucleation of *damage*; maintaining the same variational structure of [2], we develop such formulation towards a general crack model for brittle and quasi-brittle materials. In particular, to reproduce typical responses such as the strain-softening, it is well known the convenience of decomposing the strain into a part that belongs to the crack and into a part that belongs to the material (*decomposed-strain*) [6]. Here, we enrich the formulation of [2] with the possibility of considering particular inelastic deformations, associated with microstructural transformations localized in the damaged regions.

In words, when the material is damaged, its microstructure is loosened and, because of this, at the macroscopic level various types of inelastic strain become permitted in the representative volume element. The form of such a strain represents a peculiarity of the kind of material-microstructure under consideration. An effective tool to account for this possibility in the variational framework of the proposed approach is represented by Del Piero and Owen's *Structured Deformations Theory* [7]. This theory naturally decomposes the macroscopic deformation into two parts: one associated with a bulk distortion, the other one with those phenomena occurring at a lower length-scale, e.g., micro-slips, micro-cavitation etc. (the second contribution is usually referred to as the *structured part* of the deformation). We take into account various possible scenarios by considering, in the corresponding variational formulation, different classes of admissible functions to represent the structured part of the deformation. Assuming different classes, different-in-type responses can be captured, incorporating for example the ideas of cleavage, deviatoric, combined cleavage-deviatoric and masonry-like fractures.

More in particular, one may suppose that the structured part of the strain is represented by any symmetric tensor: this gives the cleavage-like fracture model discussed in Section *Cleavage fractures*. On the other hand, if the material microstructure is such that the work necessary to produce volume changes in the damaged material is much higher than that required for shear distortions, the structured part of the strain is a traceless (deviatoric) tensor: this assumption produces the deviatoric-like (mode II) fracture model of Section *Deviatoric fractures*. The resulting formulation is identical to that proposed in [2], for the case of cleavage-like fractures, and to that of [8] for the case of deviatoric fractures, respectively. In all these cases, an energetic competition is engaged between the release of elastic bulk energy and the energy necessary to produce new crack surface and, although the model takes a smeared view of the cracking phenomenon, this gives rise to strain localization in thin bands. Both these models are symmetric under tension and compression, in the sense that by reversing the sign of the external actions the crack pattern does not change, although the sign of the corresponding displacement field changes. In general, material interpenetration is not avoided, but it is at least partially mitigated in the deviatoric fracture model of the type of [8].

To overcome the somehow unrealistic symmetry under tension-compression, a combination of the two aforementioned models is also introduced, accounting for cleavage-like fractures under tension and deviatoric-like fractures under compression. This model, presented in Section *Combined cleavage-deviatoric fractures*, was obtained independently in [5] and in [9], even if from different viewpoints and with diverse purposes. Also in this case, material interpenetration is mitigated but not definitely ruled out.

A formulation that rigorously avoids material interpenetration can be obtained by imposing that the structured part of the deformation is represented by a symmetric positive-semidefinite tensor. This means that only inelastic dilatations due to micro-crack openings are permitted when the material microstructure is loosened. Remarkably, the variational approach allows to directly derive that this case, as discussed in Section *Masonry-like fractures*, is consistent with the constitutive equations for a classical masonry-like materials defined in [10], i.e., the stress tensor is negative semi-definite, coaxial and orthogonal to the structured strain. However, in the present approach, a certain mechanical work has to be consumed to open a crack, so that localized rather than smeared fractures are energetically favourable. Material interpenetration is now successfully avoided by the assumed properties of the structured part of the deformation.

The four models here presented are discussed and compared for the case of a prismatic solid under plane strain in a uniaxial tension or compression test. This is of interest because the prism may simultaneously undergo different-in-type fractures. In any case, the approach is feasible of further specialization. Just changing the form of the class of allowable structured strain, various other models, interpreting the most various responses, can be directly obtained.

THE GENERAL MODEL

If \mathcal{D} , $\mathcal{D} = 2 \div 3$, is the dimension of the Euclidean space where the problem is set, let $\Omega \in \mathbb{R}^{\mathcal{D}}$ denote the undistorted natural reference configuration of the body \mathcal{B} for which the reference frame $\{O, x_1, \dots, x_{\mathcal{D}}\}$ has been defined by the



orthogonal base of unit vectors $\{\mathbf{e}_1, \dots, \mathbf{e}_D\}$. The mapping $\mathbf{y}(\mathbf{x}): \Omega \rightarrow \mathbb{R}^D$ is the deformation so that $\mathbf{u}(\mathbf{x}) = \mathbf{y}(\mathbf{x}) - \mathbf{x}$ is the displacement of \mathbf{x} .

Structured deformation of the damaged continuum

Under assigned actions the body \mathcal{B} may damage and eventually fracture. The resulting deformation is thus the consequence of two causes: the opening of micro- or macro-cracks (*structured* part of the deformation [7]) and the distortion of the elastically bent *lamellae* delimited by the crack surfaces (*elastic* part of the deformation). We take a *smear*ed view of the phenomenon so that the corresponding strain fields can be considered continuous and regular in the representative volume element (RVE). Under the hypothesis of infinitesimal deformations, the global strain is the symmetric gradient of the displacement field, i.e., $\nabla^s \mathbf{u} = (\nabla \mathbf{u} + \nabla \mathbf{u}^T) / 2$, for which we assume a decomposition of the form

$$\nabla^s \mathbf{u}(\mathbf{x}) = \mathbf{E}_e(\mathbf{x}) + \mathbf{E}_s(\mathbf{x}) \quad (2.1)$$

where $\mathbf{E}_e(\mathbf{x})$ and $\mathbf{E}_s(\mathbf{x})$ denote the elastic and structured part of the strain, respectively. We further assume that an internal state variable $s(\mathbf{x}): \Omega \rightarrow [0,1] \subset \mathbb{R}$ is defined that represents a damage parameter that takes the 1 value in a sound zone and the 0 value in a completely damaged (fractured) zone. The significance of s is defined by the relation

$$\mathbf{E}_s(\mathbf{x}) = [1 - s(\mathbf{x})] \mathbf{E}_c(\mathbf{x}) \quad (2.2)$$

where $\mathbf{E}_c(\mathbf{x})$ represents the (structured) part of the deformation that would develop in a neighborhood of the particle \mathbf{x} if, here, the material was completely damaged, i. e., $s(\mathbf{x}) = 0$. Obviously, $s = 0$ ($s = 1$) implies $\mathbf{E}_s = \mathbf{E}_c$ ($\mathbf{E}_s = \mathbf{0}$), while s taking an intermediate value between 0 and 1 means that the material is not completely damaged and, consequently, cannot attain the whole structured strain \mathbf{E}_c that would be available in a completely disgregated RVE.

The energy

Let l represent the characteristic material length scale, i.e., the characteristic width of the process-zone band associated with the phenomenon of crack coalescence [11]. Under isothermal evolution the strain energy depends upon the displacement field $\mathbf{u}(\mathbf{x})$, the damage field $s(\mathbf{x})$ and the structured deformation field $\mathbf{E}_c(\mathbf{x})$ according to a relationship of the type

$$\Pi_l[\mathbf{u}, s, \mathbf{E}_c] = \int_{\Omega} \Psi(\nabla^s \mathbf{u}, s, \mathbf{E}_c) d\mathbf{x} + \int_{\Omega} \Gamma_l(s) d\mathbf{x} \quad (2.3)$$

where $\Psi[\nabla^s \mathbf{u}, s, \mathbf{E}_c]$ denotes the bulk part of the energy, whereas $\Gamma_l(s)$ is the surface part, which is supposed to depend upon the damage variable s and on the intrinsic material length scale l [11].

For the reasons explained at length in [8], we take for $\Gamma_l(s)$ the expression

$$\Gamma_l(s) = \frac{\gamma}{2} \left[l |\nabla s|^2 + \frac{(1-s)^2}{l} \right] \quad (2.4)$$

where γ is a parameter representative of the material fracture energy, which guarantees that the width of the bands where the strain localizes is of the same order of l .

The bulk energy is associated with the elastic part of the energy stored in the elastically deformed lamellae comprised among the microcracks. If $\mathbb{C}: \text{Sym} \rightarrow \text{Sym}$ denotes the elasticity tensor of the sound material, then

$$\Psi(\nabla^s \mathbf{u}, s, \mathbf{E}_c) = \frac{1}{2} \mathbb{C}[\mathbf{E}_e] \cdot \mathbf{E}_e$$

where \mathbf{E}_e is defined from (2.1) and (2.2). In general, if a fractured body is conveniently constrained, then the sound portions are sufficient to maintain the various pieces together. More precisely, suppose that in a small neighborhood $\omega(\mathbf{x}) \subset \Omega$ of \mathbf{x} , of the same order of the RVE, the body is completely damaged ($s(\mathbf{x}) = 0$). Let \mathbf{H} be any constant second-order tensor and consider the problem in which the boundary $\partial\omega(\mathbf{x})$ of $\omega(\mathbf{x})$ is subjected to the Dirichlet condition $\mathbf{u}(\mathbf{x}) = \mathbf{H}\mathbf{x}$, $\forall \mathbf{x} \in \partial\omega(\mathbf{x})$. Then, we define the *relaxed* bulk energy density through the expression

$$\Psi^{**} \left(\frac{\mathbf{H} + \mathbf{H}^T}{2}, s \right) \Big|_{s=0} = \inf_{\mathbf{u}, \mathbf{E}_c} \left\{ \frac{1}{V(\omega)} \int_{\omega} \Psi(\nabla^s \mathbf{u}, 0, \mathbf{E}_c) d\mathbf{x}, \mathbf{E}_c \in \mathcal{S}, \mathbf{u}(\mathbf{x}) = \mathbf{H}\mathbf{x} \text{ on } \partial\omega \right\} \quad (2.5)$$



where $V(\omega)$ denotes the measure of ω , whereas \mathbf{S} represents the admissible class for the structured part of the strain, which depends upon material properties. It should be noticed that, in general, (2.5) uniquely defines the tensor $\mathbf{E}_c = \mathbf{E}_c^{**}$ associated with the local value of the strain $\nabla^s \mathbf{u}$. We emphasize this dependence through the notation $\mathbf{E}_c^{**} = \Theta(\nabla^s \mathbf{u})$, indicating that the function $\Theta: \text{Sym} \rightarrow \text{Sym}$ associates with the local strain $\nabla^s \mathbf{u}$ the unique minimizer \mathbf{E}_c^{**} of (2.5). One can show that in the case of a linear elastic material, the problem (2.5) is indeed well posed because of the convexity of the elastic strain energy.

When $s \neq 0$, according to the assumed definition (2.2), one defines from (2.5) the relaxed bulk energy $\Psi^{**}(\nabla^s \mathbf{u}, s) = \Psi(\nabla^s \mathbf{u}, s, \Theta(\nabla^s \mathbf{u}))$. Consequently, $\Psi^{**}(\nabla^s \mathbf{u}, s)$ takes the form

$$\Psi^{**}(\nabla^s \mathbf{u}, s) = \frac{1}{2} \mathbb{C}[\nabla^s \mathbf{u} - (1-s)\Theta(\nabla^s \mathbf{u})] \cdot (\nabla^s \mathbf{u} - (1-s)\Theta(\nabla^s \mathbf{u})) \quad (2.6)$$

In conclusion, we will consider the relaxed minimization problem defined by

$$\min_{(\mathbf{u}, s) \in \mathcal{A}} \Pi_l^{**}(\mathbf{u}, s), \quad \Pi_l^{**}(\mathbf{u}, s) = \int_{\Omega} \Psi^{**}(\nabla^s \mathbf{u}, s) d\mathbf{x} + \int_{\Omega} \Gamma_l(s) d\mathbf{x} \quad (2.7)$$

where $\Pi_l^{**}(\mathbf{u}, s)$ denotes the relaxed bulk energy defined by (2.4) and (2.6), whereas \mathcal{A} represents the class of admissible functions (\mathbf{u}, s) defined according to the specific conditions for the fields $\mathbf{u}(\mathbf{x})$ and $s(\mathbf{x})$ on the boundary $\partial\Omega$ of Ω . Further conditions upon the minimization problem similar to those of [2] have to be added in order to consider irreversibility of damage. In a load history when the boundary data vary with the time t , the equilibrium state of the body are found through a sequence of minimization problems of the type (2.7), each one corresponding to a small increment of the boundary data, for which we impose that the value of s can never decrease in time.

PARTICULAR CASES

Different in type models can be obtained by considering various forms for the class \mathbf{S} of admissible structured deformation in (2.5). For the sake of brevity, in the following we only report the most important results.

Cleavage fractures

The simplest case is that in which $\mathbf{S} \equiv \text{Sym}$. Then, from (2.5) one finds that $\mathbf{E}_c^{**} = \nabla^s \mathbf{u}$ so that (2.6) reads

$$\Psi^{**}(\nabla^s \mathbf{u}, s) = \frac{1}{2} \mathbb{C}[\nabla^s \mathbf{u} - (1-s)\nabla^s \mathbf{u}] \cdot (\nabla^s \mathbf{u} - (1-s)\nabla^s \mathbf{u}) = \frac{1}{2} s^2 \mathbb{C}[\nabla^s \mathbf{u}] \cdot \nabla^s \mathbf{u} \quad (3.1)$$

Observe, in passing, that for this case one obtains for $\Pi_l^{**}(\mathbf{u}, s)$ of (2.7) an expression which is substantially similar to

$$\Pi_l^{BFM}[\mathbf{u}, s] = \int_{\Omega} \frac{1}{2} (s^2 + k_l) \mathbb{C}[\nabla^s \mathbf{u}] \cdot \nabla^s \mathbf{u} d\mathbf{x} + \frac{\gamma}{2} \int_{\Omega} \left(l |\nabla s|^2 + \frac{(1-s)^2}{l} \right) d\mathbf{x} \quad (3.2)$$

proposed by Bourdin-Francfort and Marigo [2] as a regularization of the variational formulation of Griffith's theory of [1]. The difference consists in the parameter k_l of (3.2), infinitesimal of higher order than l , which was introduced in [2] for numerical purposes but that is here irrelevant for the comparison. This model is capable to reproduce cleavage fractures, but it is symmetric in tension and compression and consequently, in general, it cannot avoid material interpenetration.

Deviatoric fractures

Let us now suppose that \mathbf{S} is the class of deviatoric, traceless, second order tensors. Having set $(\nabla^s \mathbf{u})_{sph} = \mathbf{I} \text{tr} \nabla^s \mathbf{u} / \text{tr} \mathbf{I}$ and $(\nabla^s \mathbf{u})_{dev} = \nabla^s \mathbf{u} - (\nabla^s \mathbf{u})_{sph}$, after some calculations we obtain from (2.5) that $\mathbf{E}_c^{**} = (\nabla^s \mathbf{u})_{dev}$, so that the relaxed bulk energy thus takes the form

$$\begin{aligned} \Psi^{**}(\nabla^s \mathbf{u}, s) &= \frac{1}{2} \mathbb{C}[\nabla^s \mathbf{u} - (1-s)(\nabla^s \mathbf{u})_{dev}] \cdot (\nabla^s \mathbf{u} - (1-s)(\nabla^s \mathbf{u})_{dev}) \\ &= \frac{1}{2} \mathbb{C}[(\nabla^s \mathbf{u})_{sph}] \cdot (\nabla^s \mathbf{u})_{sph} + \frac{1}{2} s^2 \mathbb{C}[(\nabla^s \mathbf{u})_{dev}] \cdot (\nabla^s \mathbf{u})_{dev} \end{aligned} \quad (3.3)$$

It is worth noticing that $\Pi_l^{**}(\mathbf{u}, s)$ of (2.7) assumes for this case an expression identical (modulo the parameter k_l) to



$$\Pi_l^{LR}[\mathbf{u}, s] = \int_{\Omega} \frac{1}{2} \left\{ \mathbb{C}[(\nabla^s \mathbf{u})_{sph}] \cdot (\nabla^s \mathbf{u})_{sph} + (s^2 + k_l) \mathbb{C}[(\nabla^s \mathbf{u})_{dev}] \cdot (\nabla^s \mathbf{u})_{dev} \right\} d\mathbf{x} + \frac{\gamma}{2} \int_{\Omega} \left(l |\nabla s|^2 + \frac{(1-s)^2}{l} \right) d\mathbf{x} \quad (3.4)$$

proposed in [8] to incorporate the idea of less brittle, “deviatoric-like” fractures.

Combined cleavage-deviatoric fractures

The models of Sections *Cleavage fractures* and *Deviatoric fractures* are symmetric in tension-compression, i.e., by reversing the sign of the boundary data one obtains exactly the same crack pattern. But experiments suggest that material response may be remarkably different in tension or compression. Consequently, one can decide to adopt the cleavage fracture model of (3.1) whenever the hydrostatic part $(\nabla^s \mathbf{u})_{sph}$ of the strain $\nabla^s \mathbf{u}$ is non-negative and the deviatoric fracture model of (3.3) when $(\nabla^s \mathbf{u})_{sph} < 0$. Reasoning as in Sections *Cleavage fractures* and *Deviatoric fractures*, one obtains for $\Psi^{**}(\nabla^s \mathbf{u}, s)$ the expression

$$\Psi^{**}(\nabla^s \mathbf{u}, s) = \begin{cases} \frac{1}{2} s^2 \mathbb{C}[\nabla^s \mathbf{u}] \cdot \nabla^s \mathbf{u}, & \text{if } (\nabla^s \mathbf{u})_{sph} \geq 0, \\ \frac{1}{2} \left\{ \mathbb{C}[(\nabla^s \mathbf{u})_{sph}] \cdot (\nabla^s \mathbf{u})_{sph} + s^2 \mathbb{C}[(\nabla^s \mathbf{u})_{dev}] \cdot (\nabla^s \mathbf{u})_{dev} \right\}, & \text{if } (\nabla^s \mathbf{u})_{sph} < 0 \end{cases} \quad (3.5)$$

For the isotropic-elasticity case, a similar model has been recently obtained independently by Amor-Marigo and Maurini [5], who proposed for the energy the expression

$$\Pi_l^{AMM}[\mathbf{u}, s] = \int_{\Omega} \frac{1}{2} \left\{ \kappa_0 \frac{(tr^-(\nabla^s \mathbf{u}))^2}{2} + (s^2 + k_l) \left[\kappa_0 \frac{(tr^-(\nabla^s \mathbf{u}))^2}{2} + \mu \nabla^s \mathbf{u} \cdot \nabla^s \mathbf{u} \right] \right\} d\mathbf{x} + \frac{\gamma}{2} \int_{\Omega} \left(l |\nabla s|^2 + \frac{(1-s)^2}{l} \right) d\mathbf{x} \quad (3.6)$$

where κ_0 and μ are the bulk and shear elastic moduli, while $tr^-(\nabla^s \mathbf{u}) = \min\{tr(\nabla^s \mathbf{u}), 0\}$ and $tr^+(\nabla^s \mathbf{u}) = \max\{tr(\nabla^s \mathbf{u}), 0\}$.

Masonry-like fractures

Let us denote by Sym^+ and Sym^- the set of all positive semidefinite and negative semidefinite symmetric tensors, respectively. The case at hand is characterized by the choice $\mathbf{S} \equiv \text{Sym}^+$ in (2.5). The detailed derivation of the function $\mathbf{E}_c^{**} = \Theta(\nabla^s \mathbf{u})$ from the minimization problem (2.5) is not reported here, but we simply recall the final results.

If $\mathbf{E} \equiv \nabla^s \mathbf{u}(\mathbf{x})$, having set $\mathbf{T}^{**} := \mathbb{C}[\mathbf{E} - \mathbf{E}_c^{**}]$, one finds that *i)* $\mathbf{E}_c^{**} \in \text{Sym}^+$; *ii)* $\mathbf{T}^{**} \in \text{Sym}^-$; *iii)* $\mathbf{E} = \mathbb{C}^{-1}[\mathbf{T}^{**}] + \mathbf{E}_c^{**}$; *iv)* $\mathbf{T}^{**} \cdot \mathbf{E}_c^{**} = 0$. These conditions imply that \mathbf{T}^{**} and \mathbf{E}_c^{**} are coaxial. Moreover, in the case of isotropic elasticity when $\mathbb{C} = 2\mu \mathbb{I} + \lambda \mathbf{I} \otimes \mathbf{I}$, being λ and μ the Lamé's elastic constants, then *v)* also \mathbf{E} is coaxial with \mathbf{T}^{**} and \mathbf{E}_c^{**} . If one establishes a correspondence between the tensor \mathbf{T}^{**} and the Cauchy stress in completely damaged body ($s = 0$), these conditions coincide with the definition of the constitutive equations for a classical linear elastic masonry like material, formulated in [10]. For any $\mathbf{E} \in \text{Sym}$ the aforementioned equations uniquely define the associated structured strain \mathbf{E}_c^{**} .

Using the property *iv)*, that is, $\mathbb{C}[\nabla^s \mathbf{u} - \Theta(\nabla^s \mathbf{u})] \cdot \Theta(\nabla^s \mathbf{u}) = 0$, one finds that (2.6) can be written in the equivalent forms

$$\begin{aligned} \Psi^{**}(\nabla^s \mathbf{u}, s) &= \frac{1}{2} \mathbb{C}[\nabla^s \mathbf{u} - \Theta(\nabla^s \mathbf{u})] \cdot (\nabla^s \mathbf{u} - \Theta(\nabla^s \mathbf{u})) + s^2 \frac{1}{2} \mathbb{C}[\Theta(\nabla^s \mathbf{u})] \cdot \Theta(\nabla^s \mathbf{u}) \\ &= (1-s^2) \frac{1}{2} \mathbb{C}[\nabla^s \mathbf{u} - \Theta(\nabla^s \mathbf{u})] \cdot (\nabla^s \mathbf{u} - \Theta(\nabla^s \mathbf{u})) + s^2 \frac{1}{2} \mathbb{C}[\nabla^s \mathbf{u}] \cdot \nabla^s \mathbf{u} \end{aligned} \quad (3.7)$$

The corresponding energy functional $\Pi_l^{**}(\mathbf{u}, s)$ results from (2.7). It can also be verified that the Cauchy stress \mathbf{T} , which is dual in energy with respect to the strain $\nabla^s \mathbf{u}$, reads

$$\mathbf{T} = (1-s^2) \mathbb{C}[\nabla^s \mathbf{u} - \Theta(\nabla^s \mathbf{u})] + s^2 \mathbb{C}[\nabla^s \mathbf{u}] = \mathbb{C}[\nabla^s \mathbf{u}] - (1-s^2) \mathbb{C}[\Theta(\nabla^s \mathbf{u})] \quad (3.8)$$

Notice that when $s = 1$ one finds the stress in a sound elastic material, whereas when $s = 0$ one obtains the expression for a classical masonry-like material [10]. There are however two major novelties here with respect to the classical no-tension theory. First, the surface-energy term (2.4) implies that the opening of fractures (i.e., s passing from 1 to 0) is associated



with an energy consumption; second, there may be regions where the material is only partially damaged (s between 0 and 1).

NUMERICAL EXPERIMENTS

We consider the paradigmatic example of a uniaxial traction or compression test of a prismatic specimen. In the following, we assume the body is a linear elastic ($\mathbb{C} = 2\mu\mathbb{I} + \lambda\mathbf{I}\otimes\mathbf{I}$) isotropic material under plain strain. Consequently, the functional of (2.7) can be properly specialized to the 2-D case.

The numerical implementation

The model is numerically implemented following the same line of [2], adding an inequality constraint on the scalar damage field s similar to that of [5] to impose crack irreversibility. The adopted numerical scheme is based upon an alternate minimization algorithm which, in short, consists in solving a series of minimization sub-problems on \mathbf{u} at fixed s and *viceversa* on s at fixed \mathbf{u} up to convergence. In particular, in the cleavage and deviatoric models of Sections *Cleavage fractures* and *Deviatoric fractures*, the energy functionals are quadratic in \mathbf{u} and the elastic sub-problem reduces to the solution of a linear system of equations. On the contrary, for the solution of the combined-cleavage-deviatoric-fractures model of Section *Combined cleavage-Cleavage fractures*, a quasi Newton algorithm is adopted because of the non-linearity induced by the inequality related to the trace of the spherical part of the strain as *per* (3.5). For the masonry-like fractures model of Section *Masonry-like fractures*, a fully Newton algorithm has been developed to obtain the equilibrium at each time step. The minimization on s at fixed \mathbf{u} is reduced to the solution of an unconstrained quadratic problem coupled with an *a posteriori* projection of the solution on the set of admissible space of s to enforce the irreversibility condition of fracture. The models have been implemented in an appositely conceived program based upon the Open Source package deal.II [12].

Examples

Consider the two-dimensional rectangular domain of Fig. 1, of sides d and b , which represents a section of the body at hand in plane strain. The element is loaded by applying a vertical displacement on the upper base Γ_2 , thus keeping equal to zero the horizontal component. The lower base Γ_1 is kept fixed while the vertical borders Γ_3 and Γ_4 are unconstrained and stress free. This setup may be representative of a tensile or compressive test with un-lubricated loading platens (perfect adhesion due to friction). To model that the contact of the loading platens strengthens the neighbouring materials, we set $s = 1$ on Γ_1 and Γ_2 . In summary, the boundary condition for this case are

$$\begin{cases} \mathbf{u} = \mathbf{0}, & s = 1, & \text{on } \Gamma_1, \\ \mathbf{u} = t\bar{u}\mathbf{e}_2, & \mathbf{u} \cdot \mathbf{e}_1 = 0 & s = 1, & \text{on } \Gamma_2, \\ \mathbf{T}\mathbf{n} = \mathbf{0}, & \nabla s \cdot \mathbf{n} = 0, & \text{on } \Gamma_3 \text{ and } \Gamma_4 \end{cases} \quad (4.1)$$

where, as in Fig. 1, \mathbf{e}_1 and \mathbf{e}_2 are the horizontal and vertical unit vectors respectively, \mathbf{n} is the outward normal to the boundary and t is the dimensionless displacement correlated with the length parameter $\bar{u} = 2.5 \cdot 10^{-4}$ mm and \mathbf{T} denotes the Cauchy stress.

We consider the case $d = 50$ mm, $b = 100$ mm, with Young's modulus $E = 30000$ N/mm² and Poisson's ratio $\nu = 0.2$. Furthermore, the fracture toughness γ has been assumed equal to $\gamma = 10^{-3}$ N/mm and the intrinsic length scale $l = 1$ mm. For what the discretization is concerned, we adopted a structured and homogeneous finite element mesh composed of 80000 quadrilaterals, with in total 3x80601 degrees of freedoms. The size of the element is $5 \cdot 10^{-3} d$, that is 0.25 l .

Figs 2-3, summarize the results obtained with the different models under traction ($t > 0$) or compression ($t < 0$). All cases are characterized by the sudden appearance of dominant cracks. In cleavage- and deviatoric-fracture models there is no difference between tension or compression, except in the sign of the displacement field.

The cleavage-fracture model of (3.1) is characterized by the appearance of two horizontal cracks (Figs. 2a and 3a) close to the lower and upper bases; the boundary condition $s = 1$ on Γ_1 and Γ_2 avoids ruptures at the constrained contours. Fractures start at the corners where the stress concentration occurs, progress and eventually meet approximately in the middle of the specimens. Their thickness, i.e., the thickness of the strip where $s \cong 0$, is of the order of l near the corners, but increases towards the center. Since the model is symmetric in tension and compression, there is no difference between Figs. 2a (traction) and 3a (compression). Obviously, material compenetration due to crack lips overlapping is not avoided under compression (Fig. 3a).

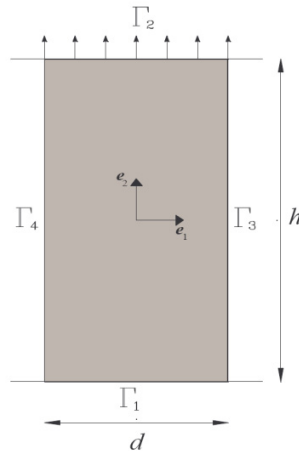


Figure 1: Section of the body in plain strain subjected to uniaxial test.

In the deviatoric-fracture model of (3.3), cracks start again at the specimen corners and propagate towards the center at an angle of approximately $\pi/4$ with respect to the horizontal. The model is again symmetric under traction and compression, presenting equal maps for the damage field. To better illustrate crack propagation, Figs. 2b and 3b represent two different stages of the load history that, even though corresponding to tension and compression tests, respectively, for the aforementioned symmetry can be considered associated with the same test. At first, two triangular wedges, with bases coinciding with Γ_1 and Γ_2 , are isolated (Fig. 2b). At this stage, a very small shear stress occurs in the middle of specimen, so that various loading steps are necessary to produce a very slow widening and propagation of cracks through a gently curved shear path, tending to separate the prism into four pieces (Fig. 3b). Notice that the model allows only for the slip and not for the opening of crack lips: consequently, the three pieces of Fig. 2b cannot separate, even if the prism is pulled. Moreover, in general the thickness of shear bands is higher than that of cleavage fractures, a phenomenon already observed in [5] and justified by the high residual stiffness of the model and bad numerical conditioning.

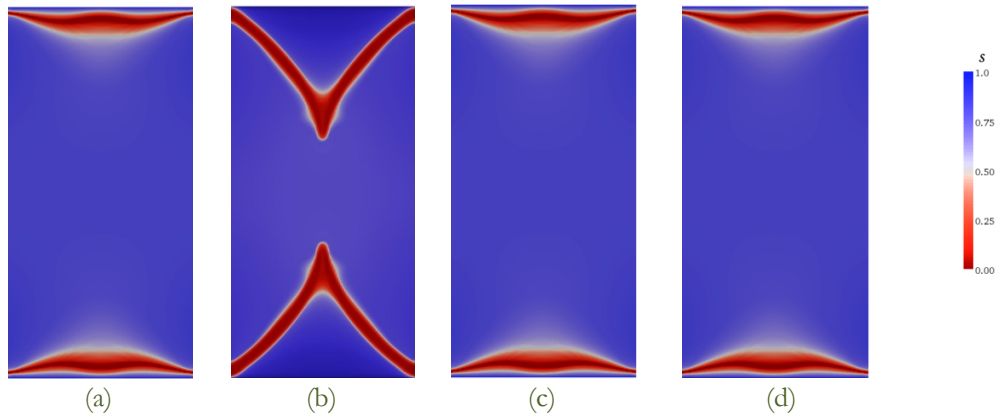


Figure 2: Uniaxial traction test ($t > 0$). Maps of s for different models: a) cleavage fracture; b) deviatoric-fracture at first loading steps; c) combined cleavage-deviatoric fracture; d) masonry-like fracture.

The combined cleavage-deviatoric fracture model of (3.5) presents under traction a crack pattern equal to that of the cleavage model (Fig. 2c), but under compression a typical hour-glass failure appears (Fig. 3c). The pseudo-vertical fracture in the middle of the specimen is a cleavage fracture provoked by the wedging action of the triangular material portions in proximity of the bases isolated by shear bands, a mechanism not allowed in the deviatoric-fracture model. Notice that also now the thickness of the shear bands is greater than the thickness of the cleavage fracture.

The masonry-like fracture model of (3.7) presents under tension horizontal fractures (Fig. 2d), again analogous to those predicted by the cleavage model. Under compression (Fig. 3d), pseudo-vertical fractures occur, which again do not reach the prism's bases Γ_1 and Γ_2 , because, here, the material is bi-axially compressed due to the confining effect. More in particular, fractures under compression manifest in two successive steps. First, the central vertical fracture appears; second, two new vertical cracks are nucleated symmetrically with respect to the prism axis (Fig. 3d). After this, the

simulation shows numerical instability. Experiments on quasi-brittle materials like geomaterials or ceramics confirm that cracks appear in a similar way, but failure is due to a second order effect, i.e., the instability of material columns comprised between fractures, that our model cannot reproduce.

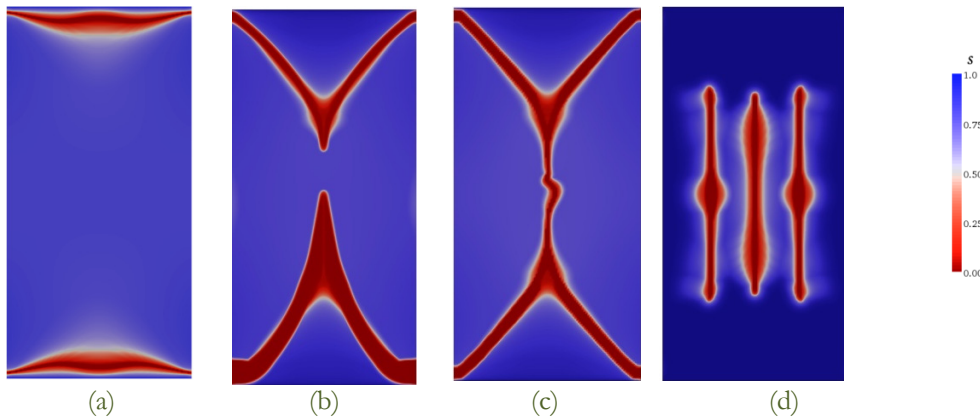


Figure 3: Uniaxial compression test ($t < 0$). Maps of s for different models: a) cleavage fracture; b) deviatoric-fracture at last loading steps; c) combined cleavage-deviatoric fracture; d) masonry-like fracture.

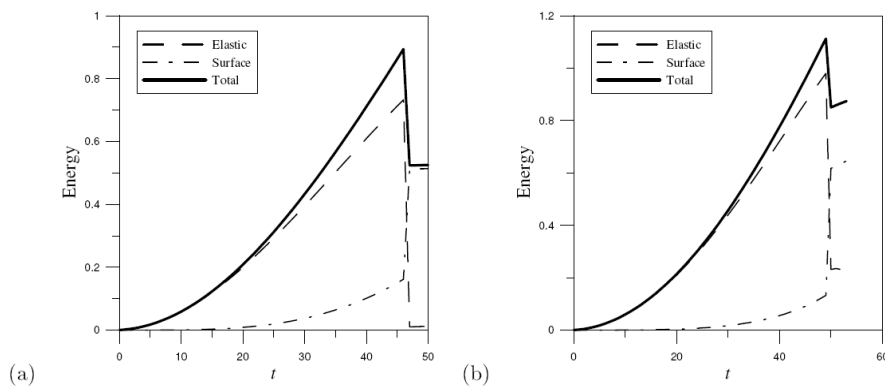


Figure 4: Uniaxial experiment: total-, bulk- and surface-energy diagrams as a function of t . a) Graphs for the cleavage-fracture model under traction $t \geq 0$ or compression $t \leq 0$ (in this case t is in absolute value) and for combined cleavage-deviatoric fracture model under traction. b) Deviatoric fracture model under traction ($t \geq 0$); the graph for the deviatoric-fracture model under compression ($t \leq 0$) is symmetrically identical.

The corresponding graphs of the total, bulk and surface energies are reported in Figs. 4 and 5 as a function of the dimensionless displacement t . Due to the energetic symmetries already discussed in Section *Examples*, Fig. 4a refers to four cases: cleavage fracture model under traction or compression (in this case t should be replaced by its absolute value); combined cleavage-deviatoric fracture model under traction; masonry-like fracture model under traction. Besides, Fig. 4b corresponds to the deviatoric fracture model under traction ($t \geq 0$) or compression ($t \leq 0$), with t identified with its absolute value. Notice the marked jumps in the total energy graphs similar to those observed, for the case of the elastic matrix with inclusion, in [5]. We agree with the conclusions of [13] and [5] that such discontinuities correspond to jumps from one local equilibrium configuration to another associated with a lower energetic level. The formation of a main fracture is evidenced by a sharp transformation of the bulk energy into surface energy. In general, the response is “stiffer” in the deviatoric-fracture model than in the cleavage fracture model.

Fig. 5 represents the energy graphs for the combined cleavage-deviatoric and the masonry-like fracture model for the uniaxial compression tests, for both of which the tensile case is represented by Fig. 4a. Also here we notice that the energy thresholds that are attained under compression are much higher than in tension, with a difference of at least one order of magnitude for the masonry like model. In particular, the graphs of Fig. 5b apparently do not indicate a visible transfer of energy from the bulk to the surface part of the energy. As a matter of fact, a magnification of the graphs in a neighbourhood of the points where the pseudo-vertical cracks of Fig. 3d appear would evidence a phenomenon of this kind, but the amount of energy that is involved is so much less than corresponding total energy level that such a



phenomenon cannot be appreciated at the scale of resolution of Fig. 5b. In conclusion, the masonry-like model naturally furnishes an interpretation of the well known evidence that brittle and quasi-brittle materials usually present strengths much higher in compression than in tension.

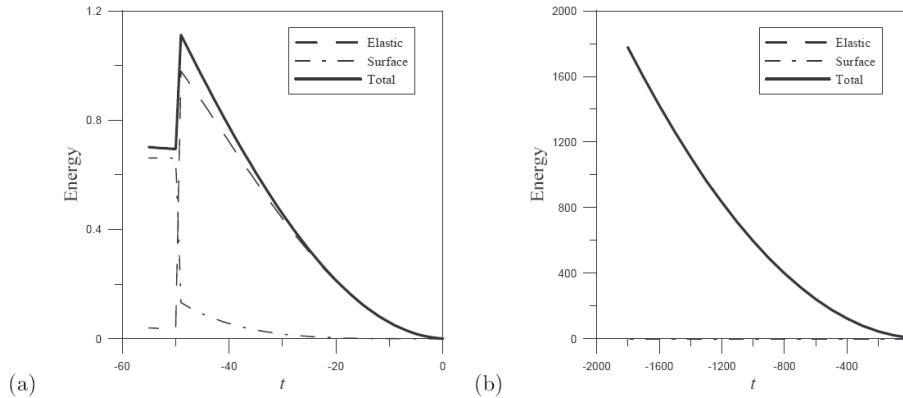


Figure 5: Uniaxial experiment under compression ($t \leq 0$): energy diagram for a) combined cleavage-deviatoric and b) masonry-like fracture models.

CONCLUSIONS

The proposed variational approach to fracture is obtained through the minimization of a two-field regularized functional that, with respect to other approaches, bypasses the difficulties associated with the discontinuities of the displacement field and the unknown crack location (free discontinuity problem). Fracture is described by a regular field measuring the damage level in the representative volume element: a crack is not a discontinuity of the displacement field, but a loosening of the microstructure and the corresponding localized weakening of the material stiffness, with the localization of large strains in very narrow bands. The model is minimal since the only required material parameters are the elastic moduli, the fracture surface energy and the material intrinsic length scale. The latter is of particular importance because this formulation is a pseudo spatial-dependent theory and this parameter influences the width of the fracture bands. The gross response of a body may be strain-softening in type due to crack opening but, locally, the material is linear elastic up to fracture: consequently, the numerical implementation results mesh-independent, not suffering the drawbacks of models with strain-softening local constitutive equations.

But the main novelty here is the combination of Structured Deformation Theory within the variational approach. We have showed in paradigmatic examples that just changing the form of the class of admissible functions for the structured strain, very different types of fracture patterns can be obtained. The corresponding micromechanics of cracking may vary between cases referred to as cleavage, deviatoric, combined cleavage-deviatoric and masonry-like fractures. Although these models take a smeared view of the cracking phenomenon, here the competition between the release of elastic bulk energy and the energy necessary to produce new crack-surface renders fracture localization energetically more favorable than diffuse cracking. Moreover, the form of the structured strain can avoid material interpenetration in the damaged zone for the case of the masonry-like fracture model.

Of course the potentiality of the approach is not limited to the four cases here considered. Further specializations to other particular material responses are allowed by consideration of other specific forms of the class of structured strains. Even if some aspects, in particular the numerical implementation, still need to be improved, the regularized variational approach to fracture mechanics seems to be a very powerful tool, whose possibility to solve practical structural problems, as pursued in [8], is yet to be fully appreciated.

ACKNOWLEDGEMENT

We are in debt with Gianpietro Del Piero for his valuable comments and helpful suggestions about a first version of this work.



REFERENCES

- [1] G. A. Francfort, J. J. Marigo, *J. Mech. Phys. Solids*, 46 (1998) 1319.
- [2] B. Bourdin, G. A. Francfort, J. J. Marigo, *J. Mech. Phys. Solids*, 48 (2000) 797.
- [3] A. Braides, *Γ -Convergence for Beginners*, Oxford University Press, Oxford (2002).
- [4] L. Ambrosio, V. M. Tortorelli, *Comm. Pure. Appl. Math.*, XLIII (1990) 999.
- [5] H. Amor, J. J. Marigo, C. Maurini, *J. Mech. Phys. Solids*, 57 (2009) 1209.
- [6] J. G. Rots, In: *Finite Elements in Civil Engineering, Third DIANA World Conference*, M. Hendrinks and J. G. Rots eds., Balkema, Lisse, (2002) 17.
- [7] G. Del Piero, D. R. Owen, *Arch. Rat. Mech. Anal.*, 124 (1993) 99.
- [8] G. Lancioni, G. Royer-Carfagni, *J. of Elasticity*, 95 (2009) 1.
- [9] F. Freddi, G. Royer-Carfagni, , In: *XIX AIMETA Symposium*, Ancona, (2009) 1.
- [10] G. Del Piero, *Meccanica*, 24 (1989) 150.
- [11] Z. Bažant, S. T. Planas, , *Fracture and Size-effect in Concrete and other Quasi-Brittle Materials*, CRC press, New York (1998).
- [12] W. Bangerth, R. Hartmann, G. Kanschat, *Deal.II, Differential Equations Analysis Library*, Technical Reference, <http://www.dealii.org> (2009).
- [13] B. Bourdin, *Interfaces and Free Boundaries*, 9 (2007) 411.